Chemical Engineering Science Vol. 37, No. 4, pp. 1007–1014, 1982
Printed in Great Britain.

0009–2509/82/071007–08$03.00/0

THERMAL EFFECTS IN NON-ADIABATIC BINARY DISTILLATION

EFFECTS OF PARTIAL CONDENSATION OF MIXED VAPORS ON THE RATES OF HEAT AND MASS TRANSFER AND PREDICTION OF H. T. U.

AKIRA ITO and KOICHI ASANO*

Department of Chemical Engineering, Tokyo Institute of Technology, Ookayama-2-chome, Meguroku, Tokyo 152,

(*Received* 15 *February* 1981; *accepted* 23 *September* 1981)

Abstract—In order to investigate thermal effects in binary distillation, theoretical approaches were made by use of a laminar boundary layer theory with uniform suction or blowing at the interface to give the following correlations for heat and mass fluxes:

$$Nu_{Gx} = 0.332\, Re_{Gx}^{1/2}\, Pr_G^{1/3}\, g(F(0), Pr_G)$$
$$Sh_{Gx}(J_{Axs}/N_{Ax}) = 0.332\, Re_{Gx}^{1/2}\, Sc_G^{1/3}\, g(F(0), Sc_G).$$

From the energy balance at the vapor–liquid interface the factors which affect interfacial velocities or $F(0)$ were discussed.

Measurements of heat and mass fluxes in a vertical flat-plate wetted-wall column for the methanol-water system were made and gave a good agreement with the theory.

A new method for the prediction of H_{OG} in binary distillation under partial condensation was proposed. The calculated H_{OG}'s gave a fairly good agreement with the observed results.

INTRODUCTION

Although binary distillation is a process of simultaneous transfer of heat and mass in which a mixed vapor contacts with its condensate, it has long been considered as a simple mass transfer process since the pioneering work of Murphree[15]. Therefore there still remain many unsolved or half-solved problems that need further discussions, among which the effect of partial condensation on the rates of mass transfer and the effect of liquid concentrations on tray efficiencies or H.T.U. are of practical importance.

The two main causes of partial condensation of a mixed vapor in distillation columns are the temperature differences between the free stream vapor and the liquid at the interface in the vapor-liquid contacting sections and the temperature differences between the inlet reflux and the bubble points of the liquid at the top of the column. Although the latter effect can be reduced by careful operation, the former is essential to distillation processes and can not be neglected in the prediction of the rates of mass transfer in the actual columns. Danckwerts[7] was the first who noticed this effect and proposed a concept of thermal distillation. Although a number of studies[5, 6, 10, 18] have been made afterwards, most of them are theoretical and are based on assumptions of which the validities have not been confirmed by experiments. Few data are known to elucidate the true mechanism of the heat and mass transfer phenomena in distillation processes.

In our previous paper[13], measurements of the heat and mass fluxes for the methanol–water and for the ethanol–water systems by a vertical flat-plate wetted-wall column at total reflux conditions were made and correlations for the vapor-phase heat and diffusion fluxes in binary distillation for relatively low degree of partial condensation or evaporation were proposed by use of a laminar boundary layer theory. The purpose of the present study is to investigate the applicability of these correlations to non-adiabatic binary distillation under high degree of partial condensation and to develope relations which predict the amount of the vapor partially condensed and rates of mass transfer in the operating conditions.

*Author to whom correspondence should be addressed.

1. THEORETICAL APPROACH

1.1 *Physical picture and fundamental equations*

Figure 1 shows a physical picture of the heat and mass transfer phenomena in binary distillation in which a reflux liquid flowing down along a vertical flat-plate contacts its vapor countercurrently. The free stream vapor- and the vapor-liquid interface temperatures are at their equilibrium values, the dew point and bubble point respectively. Since the former is higher than the latter, this temperature difference causes a transfer of sensible heat from the free stream vapor to the interface. The free stream vapor concentration of the more-volatile component (m.v.c.), A, is lower than the one at the interface and this concentration difference causes simultaneous transfer of the m.v.c. from the interface to the free stream vapor and of the less volatile component (l.v.c.) in the opposite direction. Since there is no reason these two mass fluxes should be balanced, the normal component of the velocity at the interface, v_s, is finite in binary distillation.

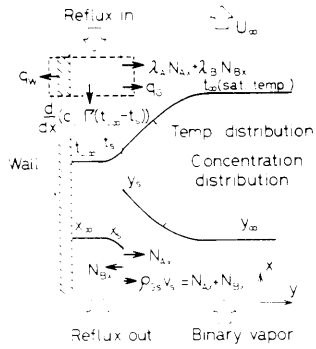

Fig. 1. Heat and mass transfer in binary distillation.

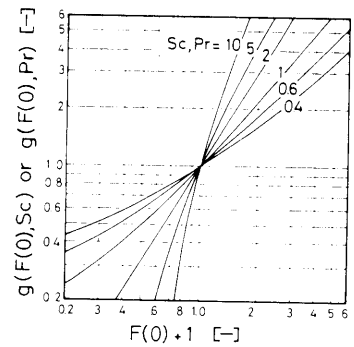

Fig. 2. Function $g(F(0), Sc)$ or $(F(0), Pr)$.

If we assume that laminar boundary layers of constant properties develop along a vertical flat plate in the vapor-phase and that these velocity-, thermal-, and concentration boundary layers are not affected by the presence of the falling liquid film and that the thickness of the liquid film is neglected in comparison with the thickness of the boundary layers, the vapor-phase transport equations can be written as:

$$F''' + (1/2)FF'' = 0 \tag{1}$$

$$\Theta'' + (Pr_G/2)F\Theta' = 0 \tag{2}$$

$$\Phi'' + (Sc_G/2)F\Phi' = 0. \tag{3}$$

The boundary conditions are:

$$F(0) = -2(v_s/U_\infty)Re_{Gx}^{1/2} \tag{4.a}$$

$$F'(0) = \Theta(0) = \Phi(0) = 0 \tag{4.b}$$

$$F'(\infty) = \Theta(\infty) = \Phi(\infty) = 1. \tag{4.c}$$

By use of a quasi-linearization method[2], numerical solutions of these equations can be obtained easily, and the vapor-phase sensible heat flux and the diffusion flux can be written as;

Heat transfer

$$Nu_{Gx} \equiv \frac{q_{Gx}x}{\kappa_G(t_s - t_{G\infty})} = 0.332\, Re_{Gx}^{1/2} Pr_G^{1/3} g(F(0), Pr_G). \tag{5}$$

Mass transfer

$$Sh_{Gx}(J_{Axs}/N_{Ax}) \equiv \frac{J_{Axs}x}{\rho_G \mathscr{D}_G(\omega_{AGs} - \omega_{AG\infty})} = 0.332\, Re_{Gx}^{1/2} Sc_G^{1/3} g(F(0), Sc_G) \tag{6}$$

where the function, $g(F(0), Pr_G)$ or $g(F(0), Sc_G)$, represents a measure of the effect of boundary layer enlargement or reduction with partial-evaporation or-condensation of a mixed vapor, of which values have been reported elsewhere[2, 8, 13, 14, 17]. Figure 2 shows numerical values of $g(F(0), Sc)$ obtained by the authors. These values were well correlated with an accuracy of better than ±1% by:

For $F(0) > 0$, $0.2 \le Sc \le 10$;

$$g(F(0), Sc) = 1 + 1.2\, Sc^{0.68} F(0)^{1.04} \tag{7a}$$

For $F(0) < 0$, $0.4 \le Sc \le 3$;

$$g(F(0), Sc) = 1 - 0.96\, Sc^{0.43} |F(0)|^{0.91}. \tag{7b}$$

1.2 *Normal component of the interfacial velocity, v_s*

A heat balance applied to a small interface element, dx, as shown in Fig. 1 gave the following equation:

$$\lambda_A N_{Ax} + \lambda_B N_{Bx} + q_{Gx} - \frac{d}{dx}\Gamma c_L(t_{L\infty} - t_s) + q_w = 0 \tag{8}$$

where q_w represents heat loss or supply through the wall.

The mass balance at the interface is also given by:

$$\rho_s v_s = N_{Ax} + N_{Bx} \tag{9}$$

$$N_{Ax} + N_{Bx} - d\Gamma/dx = 0. \tag{10}$$

Assuming that the properties are constant and that $d(t_{L\infty} - t_s)/dx = 0$, the rearrangement of eqns (8)–(10) gives the relation for the normal component of the interfacial velocity, v_s, as follows:

$$\rho_s v_s = \frac{(1 - \lambda_A/\lambda_B)}{1 - c_L(t_{L\infty} - t_s)/\lambda_B} N_{Ax} - \frac{(q_{Gx} + q_w)}{\lambda_B(1 - c_L(t_{L\infty} - t_s)/\lambda_B)}. \tag{11}$$

1.3 *Calculation of heat and mass fluxes under partial condensation or evaporation*

For mass transfer in a binary system, the general relationships between mass fluxes, N_{Ax}, N_{Bx}, and diffusion fluxes, J_{Ax}, J_{Bx}, are[1, 3]:

$$N_{Ax} = J_{Axs} + \rho_s v_s \omega_{AGs} \tag{12}$$

$$N_{Bx} = J_{Bxs} + \rho_s v_s (1 - \omega_{AGs}) \tag{13}$$

$$J_{Axs} + J_{Bxs} = 0. \tag{14}$$

By use of eqns (4a), (5), (6), (7a) and (7b) for heat and mass fluxes, eqn (11) for interfacial velocity, v_s, and eqns (12)–(14) for diffusion fluxes, numerical values of the

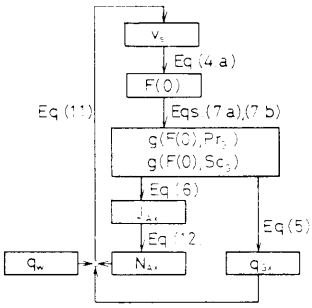

Fig. 3. Calculation of vapor-phase heat flux, mass flux and interfacial velocity in binary distillation.

vapor-phase local heat- and mass fluxes can be calculated. Figure 3 shows a flow chart for the calculation of vapor-phase heat- and mass fluxes.

If we assume that the liquid concentrations at the vapor-liquid interface is known and that the temperatures of the free stream vapor and of the interface are at their equilibrium temperatures, dew point and bubble point, respectively, we can easily calculate the axial distribution of the free stream vapor concentrations along the wetted-wall only from top ($x_{\infty 2}$, $y_{\infty 2}$, Γ_2, $U_{\infty 2}$) or bottom conditions ($x_{\infty 1}$, $y_{\infty 1}$, Γ_1, $U_{\infty 1}$). So, the number of transfer units or H.T.U. can be calculated by the following equations:

$$N_{OG} \equiv \int_{y1}^{y2} \frac{dy}{y^* - y} \tag{15}$$

$$H_{OG} \equiv Z/N_{OG}. \tag{16}$$

The partial condensation ratio is given by:

$$\beta = 1 - \Gamma_2/\Gamma_1 \tag{17}$$

Equation (5), (6) and (8) were compared with the data in the later discussions.

2. EXPERIMENTAL APPARATUS AND PROCEDURES

2.1 *Experimental apparatus*

Figure 4 shows a schematic diagram of an experimental apparatus. The test section, which was almost similar to that used in the previous work[13], was a vertical flat-plate type wetted-wall column with a 18 mm-wide, 196 mm-long vapor–liquid contacting area. On the reverse side of the wetted-wall plate, a flow of cooling water was arranged to control the surface temperatures of the wetted-wall. On the opposite side of the wetted-wall, two 0.25 mm–o.d. sheathed Chromel–Alumel thermocouples, 76 mm and 156 mm from the lower edge of the wetted-wall, respectively, were mounted on separate traversing mechanisms for measurements of the vapor-phase temperature profiles.

In order to confirm the validity of the flow pattern in the test section, preliminary measurements of the velocity- and temperature profiles for the cooling of air were made. The data showed good agreement with the

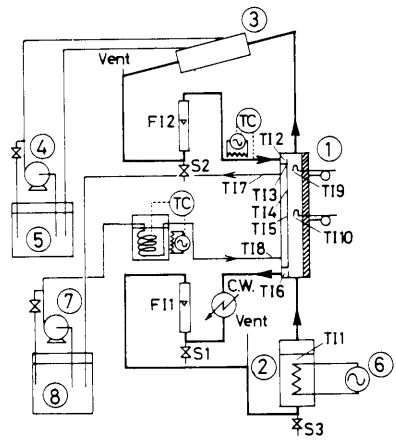

Fig. 4. Schematic diagram of experimental apparatus; (1) test section, (2) still, (3) total condenser, (4) and (7) pump, (5) and (8) water reservoir, (6) variable heater: (TI) thermocouple for (1) still temp., (2) and (6) reflux inlet- and outlet-temp., (3) (4) (5) wall temp., (7) and (8) cooling water inlet- and outlet-temp., (9) and (10) vapor-phase temperature profile: (S1) (S2) (S3) sampling tap: (FI1) and (FI2) rotameter for outlet- and inlet-liquid.

theoretical values obtained by a laminar boundary layer theory[13].

2.2 *Measurements*

Measurements were made for the methanol–water system at total reflux conditions with different liquid concentrations, vapor flow rates and partial condensation ratios. The temperature differences between the bubble points of the inlet reflux and the temperatures of the actual inlet reflux were kept within 5°K throughout this work. The rates of partial condensation of the binary vapor were varied by adjusting the temperatures of the cooling water several degrees lower than the bubble points of the inlet reflux liquid.

The top- and bottom-reflux flow rates, Γ_2 and Γ_1, were measured by two precision-type rotameters with an accuracy of about 1%. The top- and bottom-reflux concentrations of the m.v.c., ω_{AL2} and ω_{AL1}, were measured by a precision-type refractometer with an accuracy of about 0.1 mol%. From these measurements, the mass fluxes of the more- and the less-volatile component, N_A and N_B, were determined by:

$$\bar{N}_A = (\Gamma_2\omega_{AL2} - \Gamma_1\omega_{AL1})/Z \tag{18a}$$

$$\bar{N}_B = \{\Gamma_2(1-\omega_{AL2}) - \Gamma_1(1-\omega_{AL1})\}/Z. \tag{18b}$$

The vapor-phase sensible heat fluxes, q_{Gx}, were evaluated by means of the least-square method from the vapor-phase temperature profiles by;

$$q_{Gx} = -\kappa_G(\partial t/\partial y)_{y=\delta,ob} \tag{19}$$

where the temperature gradients at the interface were evaluated by numerical differentiation of the profile data with respect to y.

The interfacial velocity, v_s, and values of $F(0)$ and $g(F(0), Sc_G)$ were evaluated by the same method as

described in the previous work[13]:

$$\bar{v}_s = (\Gamma_2 - \Gamma_1)/\rho_s Z \tag{20}$$

$$\overline{F(0)} = \int_0^Z F(0)\,dx = -(4\bar{v}_s/3U_\infty)\,Re_G^{1/2} \tag{21}$$

$$g = g(\overline{F(0)}, Sc_{Gs}). \tag{22}$$

Reynolds numbers were evaluated in terms of the center velocities of the duct (maximum velocity) and the distance from the lower edge of the wetted-wall. The validity of this procedure has already been discussed in the previous paper[13].

Vapor-liquid equilibrium of the system was evaluated from the vapor pressures by Antoine's equations and from the activity coefficients by Wilson's equations, where properties constants by Holmes and van Winkle[12] were used. The viscosities and the thermal conductivities of the mixed vapor were estimated by Wilke's method. The binary diffusion coefficients and the viscosities of the pure vapors were estimated by Hirschfelder's method. The vapor-phase Schmidt- and Prandtl-numbers were evaluated at the vapor–liquid interface.

3. EXPERIMENTAL RESULTS AND COMPARISON WITH THE THEORY

3.1 *Vapor-phase temperature profiles and separation of the individual resistances*

Figure 5 shows an example of the vapor-phase temperature profiles at the same reflux liquid concentrations and vapor Reynolds numbers, Re_G, but at different partial condensation ratios, β. A regular decrease in the thickness of the thermal boundary layer with increase in partial condensation ratios was observed. The theoretical temperature profiles calculated from eqn (2) by a quasi-linearization method[2] also showed a good agreement with the data.

The observed free stream vapor temperatures, $t_{G\infty}$, agreed very well with the dew points of the free stream vapor concentrations, t_d, which were higher than the interface temperatures. The observed interface temperatures, t_{sob}, obtained by extraporating the profile data to the interface ($y \simeq 0.1$ mm) also agreed very well with the bubble points of the liquids at the interface, of which concentrations, x_s, were calculated from the observed bulk liquid concentrations, x_∞, by use of Higbie's penetration theory:

$$k_c Z/\mathscr{D}_L = 1.693(\Gamma/\rho_L\mathscr{D}_L)\sqrt{p} \tag{23}$$

$$p \equiv \mathscr{D}_L Z/\delta^2 U_{L,s} \tag{24}$$

$$x_s = x_\infty - (\bar{J}_A/M_A)/ck_c. \tag{25}$$

On the basis of these observations, the interfacial vapor concentrations of the m.v.c., y_s, which were necessary for the later discussions, were taken equal to the equilibrium concentrations at observed interface temperatures obtained by temperature measurements, t_{sob}.

Figure 6 shows the effect of vapor condensation (β) on the relative order of magnitude of the vapor-phase mass transfer driving force, $(y_{sob} - y_\infty)/(y^* - y_\infty)$. Although a slight decrease in vapor-phase mass transfer driving force with increase in β and with decrease in the liquid concentration was observed, the vapor-phase resistances were found to take a major role in binary distillation.

3.2 *The effect of partial condensation of the rates of heat and mass transfer*

Figure 7(a) shows the experimental results for the vapor-phase heat fluxes obtained by temperature measurements, where a solid line represents the results of theoretical calculations by eqn (5) for $\beta = 0$ ($F(0) = 0$). As was expected from the discussions in the previous sections, a considerable effect of partial condensation was observed. In Fig. 7(b), the local Nusselt numbers corrected for the effect of partial condensation by use of eqns (7a) or (7b), were plotted against local Reynolds numbers, Re_{Gx}, and show a good agreement with the theory, where a solid line shows the results of theoretical calculations by eqn (5).

Figure 8 shows the effect of partial condensation on the mass fluxes, $\bar{N}_A$ and $\bar{N}_B$, the diffusion fluxes of the m.v.c., $\bar{J}_A$, and the interfacial velocities, $\bar{v}_s$, at nearly the same Reynolds numbers and mass transfer driving forces, where a comparison was made for the same data used in Fig. 5. As is the case for the heat fluxes, the diffusion fluxes of the m.v.c., $\bar{J}_A$, increase with increase of partial condensation ratio, β. The mass fluxes of the m.v.c., $\bar{N}_A$, decrease with increase of β and become negative for large values of β, where a transfer of the

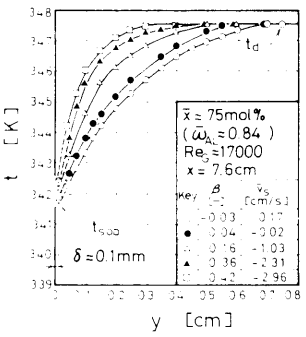

Fig. 5. Effect of partial condensation on vapor-phase temperature profile.

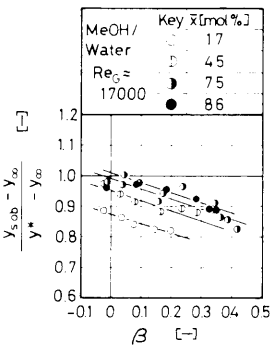

Fig. 6. Vapor-phase mass transfer resistance; Relation between $(y_{sob} - y_\infty)/(y^* - y_\infty)$ and β.

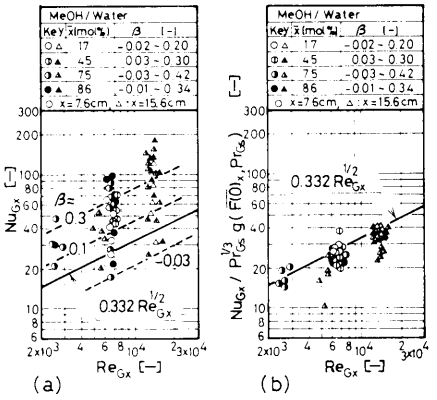

Fig. 7. Vapor-phase heat flux; (a) Relation between Nu_{Gx} and Re_{Gx}, (b) Relation between $Nu_{Gx}/Pr_{Gs}^{1/3}\ g(F(0), Pr_{Gs})$ and Re_{Gx}.

m.v.c. takes place from the free stream vapor to the interface although the concentrations of the m.v.c. at the interface are larger than the ones at the free stream vapor. An explanation for this phenomenon may be due to the fact that the mass fluxes are defined as algebraic sum of the diffusion fluxes and the convective fluxes caused by interfacial velocities, $\rho_s v_s \omega_{As}$, and that the amount of the m.v.c. transferred by the former fluxes is smaller than the one by the latter.

Figures 9-a, -b and -c show the experimental results for the vapor-phase mass fluxes. In Fig. 9(a), the dimensionless mass fluxes of the m.v.c., Sh_G, where plotted against the average vapor-phase Reynolds numbers, Re_G, to show an irregular scattering of the data, where negative values of the Sherwood numbers indicate transfer of the m.v.c. in an opposite direction that expected from the driving force. As was expected from Fig. 7(b), a correlation in terms of the dimensionless diffusion fluxes, $Sh_G(J_A/N_A)$, showed a better correlation although the effect of the partial condensation was also observed (Fig. 9(b)). The dimensionless diffusion fluxes corrected for the effect of partial condensation showed a good agreement with the theory. Figure 9(c) shows results of the correlation, where a solid line represents the theoretical values by eqn (6). From the facts described above, we may conclude that the eqns (5) and (6) are applicable to the vapor-phase heat and mass transfer in binary distillation under a high degree of partial condensation.

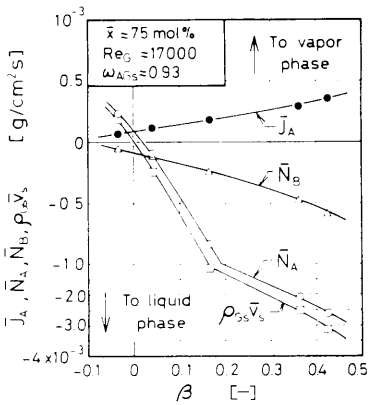

Fig. 8. Effect of partial condensation on vapor-phase mass transfer fluxes.

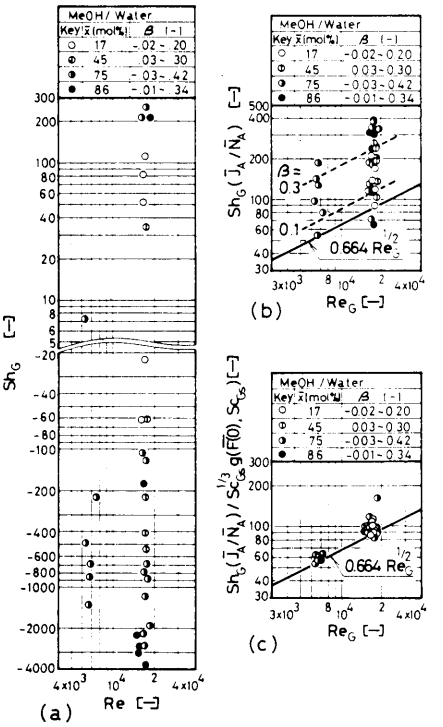

Fig. 9. Vapor-phase mass flux; (a) Relation between Sh_G and Re_G, (b) Relation between $Sh_G(J_A/N_A)$ and Re_G, (c) Relation between $Sh_G(J_A/N_A)/Sc_{Gs}^{1/3}g(F(0), Sc_{Gs})$ and Re_G.

3.3 *Energy balance at the vapor–liquid interface*

From eqns (8) and (10), the energy balance at the vapor–liquid interface can be written as:

$$N_{Ax}(\lambda_A - c_L(t_{L\infty} - t_s)) + N_{Bx}(\lambda_B - c_L(t_{L\infty} - t_s)) + q_{Gx} + q_w = 0. \quad (26)$$

Since all the terms in the above equation can easily be evaluated from direct measurements (N_A, N_B, q_{Gx}, q_w), a comparison was made in Fig. 10 by assuming that heat loss through the wall, q_w, was equal to that recieved by cooling water (q_{wob}):

$$q_w \simeq q_{wob} = c_c(t_{c2} - t_{c1})Q_c/S \quad (27)$$

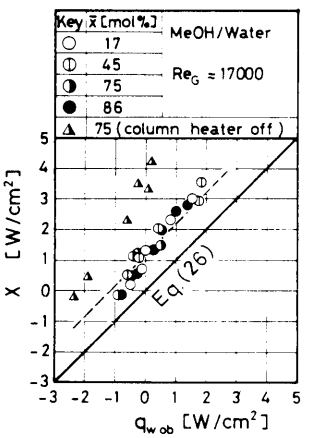

Fig. 10. Energy balance at vapor-liquid interface; A comparison with data and eqn (26).

where X was an algebraic sum of the first three terms:

$$X = -\bar{N}_A(\lambda_A - \overline{c_L(t_{L\infty} - t_s)}) - \bar{N}_B(\lambda^B - c_L(t_{L\infty} - t_s)) - \bar{q}_{Gx}. \quad (28)$$

Although the data showed a similar dependence of X on q_w as that predicted by the theory, small positive deviations from eqn (26) were observed. A possible explanation for this deviation may be due to poor thermal insulation of the test section. In order to confirm this experimentally, another series of measurements were made under the conditions where column heaters for the thermal insulation were switched off ($\blacktriangle$), to give much larger deviations.

4. DISCUSSIONS

4.1 *Effect of partial condensation on H.T.U.*

Figure 11 shows the effect of the partial condensation ratio, β, on H_{OG} for the methanol–water system by the authors at nearly same Reynolds numbers ($Re_G \simeq 1700$) but at different liquid concentrations, where the solid line shows the theoretical values obtained by the present method described in the previous sections (or Fig. 3) with an assumption of negligible effect of the liquid-phase mass transfer resistances ($x_s = x_\infty$).† The data showed a good agreement with the theory except those for $\bar{x} = 75$ mol%. The facts that H_{OG} increases with β for the low liquid concentration range (Figs. 11a and 11b) but decreases for higher concentration ranges (Fig. 11d) are worthy of note.

In Fig. 12, data for the benzene-*n*-heptane system obtained in a 3 cm-diameter packed column by Blass and Sauer[4] were compared with calculated results obtained by the present method. The abscissa of the figure is a measure of partial condensation proposed by Hochgesand[11] and is in proportion to the partial condensation ratio, β. Agreement between the data and the theory is also very good. This may indicate that the present model is also applicable to the calculation of the packed column distillation.

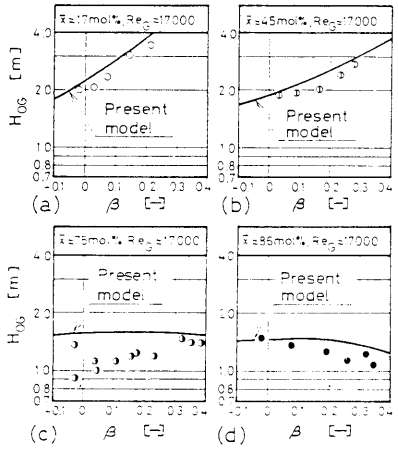

Fig. 11. Effect of partial condensation on H_{OG}; A comparison with the present model and the author's data (methanol–water system at total reflux).

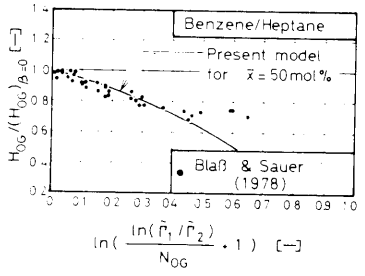

Fig. 12. Effect of partial condensation on H_{OG}; A comparison with present model ($Re_G = 1000$, $Z = 20$ cm) and the data for benzene–heptane system by Blass and Sauer[4].

4.2 *Effect of liquid concentration of H_{OG}*

Many papers on binary distillation report about the effect of liquid concentrations on mass transfer but until now no satisfactory explanation has been given for this phenomenon. In Figs. 13(a) and (b) the data for the methanol-water and for the *n*-propanol–water systems obtained with a disk column by Norman *et al.*[16] were compared with the results calculated by the present method in terms of H_{OG} for the effect of the liquid concentrations. Sample calculations were made at the conditions of $q_w = 0$, $Re_G = 1600$, $Z = 20$ cm‡ by taking into account the effect of the liquid-phase mass transfer

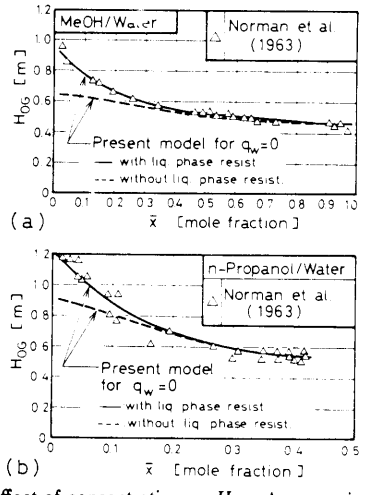

Fig. 13. Effect of concentration on H_{OG}; A comparison with the present model ($Re_G = 1600$, $Z = 20$ cm) and the data by Norman *et al.*[16], (a) methanol-water system, (b) *n*-propanol-water system.

†As is shown in Fig. 6, the effect of liquid-phase resistances in this system can be neglected in comparison with those in the vapor-phase.

‡Since the flow pattern in a disk column is quite different from that in the present apparatus, the use of eqns (5) and (6) for the calculation of the heat and diffusion fluxes in the disk column may seem questionable. In order to clear up this ambiguity, a series of calculations were made at the conditions of different Re_G and Z but these show a similar dependence of H_{OG} on the liquid concentrations, among which the best fit was shown in Fig. 13 as an example.

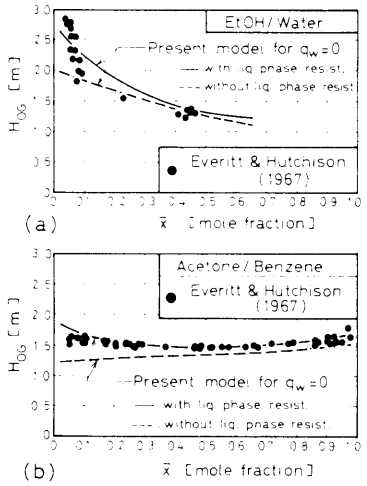

Fig. 14. Effect of concentration on H_{OG}; A comparison with the present model (Re_G = 10000, Z = 20 cm) and the data by Everitt and Hutchison[9], (a) ethanol–water system, (b) acetone–benzene system.

resistances by use of eqns (23)–(25) (solid line) and also at the same conditions without liquid-phase resistances (dotted line). Although the two calculations gave fairly good agreement with the data for the intermediate-to-high concentration ranges, better agreements were observed for that with liquid-phase resistances.

Figure 14(a) and (b) show comparisons with the data for the ethanol–water and for the acetone–benzene systems by a 2.54 cm-diameter ordinary wetted-wall column by Everitt and Hutchison[9], where the calculations were made at the conditions of $q_w = 0$, $Re_G = 10000$, Z = 20 cm.† The effect of liquid concentration on H_{OG} in binary distillation may be predicted by the present model by taking into account the liquid-phase resistances.

CONCLUSIONS

In order to investigate the effect of partial condensation of mixed vapors in binary distillation, both theoretical and experimental approaches were made to give the following results.

(1) By use of laminar boundary layer theory with uniform suction or blowing at the interface, theoretical solutions for the heat and mass fluxes under partial condensation, eqns (5) and (6), were proposed.

(2) By use of energy balance at the vapor–liquid interface the factors which affect interfacial velocities, v_s, were discussed.

(3) Measurements of heat and mass fluxes in a vertical flat-plate wetted-wall column for the methanol–water systems gave good agreement with the theory.

(4) Liquid phase resistances estimated from temperature measurements showed good agreement with the theoretical value obtained from Higbie's model.

(5) A new method for the prediction of H_{OG} in binary distillation under partial condensation was proposed. Comparisons showed good agreement with the present data and with that of previous workers.

†Same reason as is the case for disk column.

NOTATION

c molar density of the liquid, kmol/m^3; specific heat at constant pressure, J/(kg · K)
$\mathscr{D}$ binary diffusion coefficient, m^2/s
F dimensionless stream function ($\equiv \psi/\sqrt{(\nu x U_\infty)}$
g function defined by eqns (5) or (6)
H_{OG} over-all vapor-phase height of a transfer unit (eqn 16), m
J_i diffusion flux of the ith component, kg/(m^2 · s)
k_c liquid-phase mass transfer coefficient, m/s
M molecular weight, kg/kmol
N_{OG} over-all vapor-phase number of transfer units (eqn 15)
N_i mass flux of the ith component, kg/(m^2 · s)
Nu_{Gx} vapor-phase local Nusselt number ($\equiv q_{Gx}x/\kappa_G(t_s - t_{G\infty})$
p parameter defined by eqn (24)
Pr Prandtl number ($\equiv c\mu/\kappa$)
Q_c cooling water flow rate, kg/s
q_G vapor-phase sensible heat flux, W/m^2
q_w heat flux through the wall, W/m^2
Re_G Reynolds number ($\equiv \rho U_\infty Z/\mu$)
Re_{Gx} local Reynolds number ($\equiv \rho U_\infty x/\mu$)
S vapor-liquid contacting area, m^2
Sc Schmidt number ($\equiv \mu/\rho\mathscr{D}$)
Sh_G average Sherwood number ($\equiv \bar{N}_A Z/\rho_G \mathscr{D}_G(\omega_{AGs} - \omega_{AG\infty})$)
Sh_{Gx} local Sherwood number ($\equiv N_{Ax}x/\rho_G\mathscr{D}_G(\omega_{AGs} - \omega_{AG\infty})$)
t temperature, K
U_∞ free stream vapor velocity, m/s
U_{Ls} surface velocity of the liquid film, m/s
u x-component of velocity, m/s
v y-component of velocity, m/s
X parameter defined by eqn (28), W/m^2
x distance from the lower edge of the wetted-wall, m; liquid-phase mole fraction of the more volatile component
y distance from the liquid surface, m; vapor-phase mole fraction of the more volatile component
y^* vapor-phase mole fraction of the more volatile component in equilibrium with the liquid main stream (x_∞)
Z length of the wetted-wall, m

Greek symbols

β ratio of condensed vapor to inlet vapor defined by eqn (17)
Γ liquid mass flow rater per unit perimeter, kg/(m · s)
$\tilde{\Gamma}$ liquid molar flow rate per unit perimeter, mol/(m · s)
δ thickness of the liquid film, m
η similarity variable ($\equiv y\sqrt{(U_\infty/\nu x)}$
Θ dimensionless temperature ($\equiv (t - t_s)/(t_{G\infty} - t_s)$)
κ thermal conductivity, J/(m · s · K)
λ latent heat of vaporization, J/kg
μ viscosity, kg/(m · s)
ν kinematic viscosity, m^2/s
ρ density, kg/m^3

Φ dimensionless concentration ($\equiv (\omega_{AG} - \omega_{AGs})/(\omega_{AG\infty} - \omega_{AGs})$)
ψ stream function, m^2/s
ω_A mass fraction of the more volatile component

Subscripts

A more volatile component
B less volatile component
c cooling water
d dew point
G vapor phase
L liquid phase
ob observed value
s vapor-liquid interface
w wall
∞ vapor free stream or liquid main stream
1 bottom of the column
2 top of the column

Superscript

$[-]$ average with respect to coordinate x

REFERENCES

[1] Asano K., *Busshitsu Ido-Ron*, p. 12. Kyoritsu Shuppan, Tokyo 1976.
[2] Asano K., Nakano Y. and Inaba M., *J. Chem. Engng Japan* 1979 **12** 196.
[3] Bird R. B., Stewart W. E. and Lightfood E. N., *Transport Phenomena*, p. 496. John Wiley, New York 1960.
[4] Blass E. and Sauer H., *Chem. Ing.-Technik* 1978 **50** 525.
[5] Brusset H., Peuscet J. and Levain J. C., *Br. Chem. Engng* 1963 **8** 746.
[6] Byron E. S., Bowman J. R. and Coull J., *Ind. Engng Chem.* 1951 **43** 1002.
[7] Danckwerts P. V., Smith W. and Sawistowski H., *International Symposium on Distillation*, p. 7. Institution of Chemical Engineers, London 1960.
[8] Evans H. L., *Int. J. Heat Mass Transfer* 1961 **3** 321.
[9] Everitt C. T. and Hutchison H. P., *Trans. Inst. Chem. Engrs* 1967 **45** T9.
[10] Hempel J., *Chem.-Ing.-Technik*, 1967 **39** 1136.
[11] Hochgesand G., *VDI-Forschungsheft* **498**, 1963.
[12] Holmes M. J. and van Winkle M., *Ind. Engng Chem.* 1970 **62** 21.
[13] Ito A. and Asano K., *Kagaku Kogaku Ronbunshu*, 1980 **6** 352 *Heat Transfer Japanese Research* 1980 **9** 38.
[14] Kays W. M., *Convective Heat and Mass Transfer*, p. 316. McGraw-Hill, New York 1966.
[15] Murphree E. V., *Ind. Engng Chem.* 1952 **17** 747.
[16] Norman W. S., Cakaloz T., Fresco A. Z. and Sutcliffe D. H., *Trans. Inst. Chem. Engrs* 1963 **41** 61.
[17] Rose J. W., *Int. J. Heat Mass Transfer* 1979 **22** 969.
[18] Sawistowsky H., Bainbridge G. S., Stacy M. J. and Theobald A., *Distillation-Final Report by ABCM/BCPMA Distillation Panel*, p. 143. Chemical Industries Association, London 1964.